European Journal of Pediatrics (2025) 184:290
https://doi.org/10.1007/s00431-025-06134-4

RESEARCH

Global burden of pediatric urolithiasis: A trend and health inequalities analysis from 1990 to 2021

Zheng Xu[1] · Tianfu Ding[1] · Daxun Luo[1] · Yang Chen[1] · Yubao Liu[1] · Haifeng Song[1] · Boxing Su[1] · Bo Xiao[1] · Jianxing Li[1]

Received: 25 November 2024 / Revised: 2 April 2025 / Accepted: 6 April 2025

Abstract

This research seeks to evaluate the worldwide burden, health inequities, and projected trends of pediatric urolithiasis from 1990 through 2021. We calculated age-standardized incidence rates, prevalence rates, and disability-adjusted life years rates from the 2021 Global Burden of Disease database. Joinpoint regression was applied for time-trend analysis. Health disparities were measured by using Spearman correlation analysis, Relative Concentration Index, and Slope Index of Inequality. Bayesian Age-Period-Cohort models predicted future global age-standardized incidence rates trends. Global age-standardized incidence rates declined from 79 (95% confidence interval [CI], 38–132) cases per 100,000 population in 1990 to 75 (95% CI, 37–124) cases per 100,000 in 2021, although the total number of cases rose. Age-standardized incidence rates decrease sharper in high Socio-Demographic Index regions. Geographical differences reveal significant health disparities, with age-standardized disability-adjusted life years rates higher in countries with a low Socio-Demographic Index. Bayesian Age-Period-Cohort models forecast a slight rise in global age-standardized incidence rates.

Conclusions: While global age-standardized incidence rates for pediatric urolithiasis have shown a downward trend, the increasing number of cases and persistent age-standardized disability-adjusted life years rates burden in low-SDI regions underscore pressing concerns. Efforts focused on prevention, early detection, and equitable access to healthcare are critical to bridging these gaps and improving global outcomes.

What is Known:

- *Pediatric urolithiasis imposes a significant global burden, with higher recurrence rates and long-term impacts on kidney function.*
- *The incidence of urolithiasis in children varies greatly in different countries or regions around the world.*

What is New:

- *This study provides the comprehensive analysis of global trends and health inequalities in pediatric urolithiasis from 1990 to 2021 using GBD 2021 data.*
- *Persistent inequalities remain, with disadvantaged regions bearing heavier burdens despite global improvements.*

Keywords Global burden of disease · Urolithiasis · Incidence · Prevalence · Disability adjusted life-years · Age-standardized rate

Abbreviations

AAPC	Average Annual Percent Change
ACI	Absolute Concentration Index
ASIR	Age-Standardized Incidence Rate
ASR	Age-Standardized Rate
BAPC	Bayesian Age-Period-Cohort
CIs	Confidence Intervals
CT	Computed Tomography
DALYs	Disability-Adjusted Life Years Rates
ESWL	Extracorporeal shock wave lithotripsy
GATHER	Accurate and transparent health estimates reporting

Communicated by Gregorio Milani

✉ Bo Xiao
xba00975@btch.edu.cn

✉ Jianxing Li
lijianxing2015@163.com

[1] Department of Urology, Beijing Tsinghua Changgung Hospital, School of Clinical Medicine, Tsinghua University, Beijing 102218, China

Published online: 11 April 2025

GBD	Global burden of disease
GHDx	Global health data exchange
ILNA	Iterative leave-out-node approach
PC	Penalized complexity
PCNL	Percutaneous nephrolithotomy
RCI	Relative concentration index
RIRS	Retrograde intrarenal surgery
RW2	Second-order random walk
SII	Slope index of inequality
SDI	Socio-demographic index
UI	Uncertainty interval
YLLs	Years of life lost
YLDs	Years lived with disability

Introduction

Urolithiasis is an increasingly recognized public health concern, with a rising incidence reported across various age groups worldwide. Once considered predominantly an adult disease, recent epidemiological trends indicate a significant surge in pediatric cases, suggesting a shifting disease burden that warrants closer examination[1–3].

Pediatric urolithiasis presents distinct clinical and public health challenges due to its potential for recurrent stone formation, long-term renal complications, and increasing prevalence[4]. These challenges are further complicated by significant regional variations, likely influenced by metabolic risk factors, dietary patterns, obesity, and climate change[2, 5]. However, the impact of these factors is not uniform but rather shaped by geographic, genetic, and socioeconomic contexts[6], further exacerbating disparities in disease burden across regions[7–9].

To assess the broader disease burden, the Global Burden of Disease (GBD) study provides a comprehensive framework for assessing disease burden across various regions, age groups, and socioeconomic contexts. Recent analyses reveal a 26.7% increase in global urolithiasis cases from 2000 to 2021 across all age groups, with significant variations between high-income and low-income regions[10]. However, while studies have significantly advanced our understanding of urolithiasis as a global public health issue, they primarily examine the disease across all age groups, often without a focused analysis of pediatric cases.

Understanding the global trends and disparities in pediatric urolithiasis is essential for developing targeted public health interventions. This study aims to analyze the global, regional, and national burden of urolithiasis in children aged 0–14 years using GBD data, with a particular focus on incidence trends, disability-adjusted life years, and socioeconomic inequalities. By elucidating these patterns, we seek to inform policies that address underlying risk factors and enhance healthcare accessibility for affected pediatric populations worldwide.

Materials and methods

Our study complies with the Guideline for Accurate and Transparent Health Estimates Reporting (GATHER) recommendations (Supplementary Materials S3).

Data sources and extraction

This study is part of the Global Burden of Disease Study 2021, which provides comprehensive estimates of disease burden for 371 diseases and injuries across 204 countries and territories. GBD 2021 quantifies incidence, prevalence, mortality, years of life lost (YLLs), years lived with disability (YLDs), and disability-adjusted life years (DALYs) for 25 distinct age groups, stratified by sex and Socio-Demographic Index (SDI) [8, 9].

Data for this study were manually retrieved from the Global Health Data Exchange (GHDx) query tool (available at https://ghdx.healthdata.org/gbd-2021). We extracted pre-processed estimates of incidence, prevalence, and disability-adjusted life years (DALYs) for pediatric urolithiasis, stratified by age (< 5 years, 5–9 years, 10–14 years), sex, year (1990–2021), and location (5 socio-demographic index super regions, 21 subregions, and 204 countries/territories). Data were independently extracted by two authors and subsequently verified by two additional authors. Manual cross-checking was conducted to compare key variables including age groups, diseases, locations, and years between datasets. In addition, consistency checks were performed using custom scripts to ensure the reliability of the extracted data. The dataset included absolute counts and rates (per 100,000 population), along with 95% uncertainty intervals (UIs) and SDI values. No additional data cleaning or handling of missing data was performed, as the GBD 2021 database provides quality adjustments and imputations applied by the GBD collaborative team[11].

Definition of the urolithiasis

In GBD 2021, urolithiasis was identified according to the International Classification of Diseases (ICD), Tenth Revision (ICD- 10), and ICD- 9. Urolithiasis was defined as the formation of stone anywhere along the genitourinary tract (coded as N20–N23.0, 592–592.9, 594–594.9)[12].

Data calculation

For the raw GBD data, uncertainty intervals (UIs) were provided to account for variability and measurement uncertainty

in the original estimates. The 95% UIs were derived from the 25 th and 975 th percentiles of 1,000 draws, representing the range of plausible values. GBD studies draw on a wide array of data sources and models, so uncertainty stems not only from sampling error (which is addressed by confidence intervals, or CIs) but also from factors such as data quality, model assumptions, and parameter estimates.

The 0–14 age group age-standardized rates (ASRs) were obtained using data from < 5 years, 5–9 years, and 10–14 years, combined with the ageadjust.direct function from the epitools package in R[13, 14]. The 2021 GBD global standard population was used as the reference population[12]. The 95% confidence intervals (CIs) for the ASRs were calculated using the gamma distribution method to account for the uncertainty in the estimates[15]. Although the original GBD estimates include 95% UIs that incorporate a broader range of uncertainty sources such as model-based and data input variability, the ASRs in this study were derived from GBD point estimates using standard epidemiological procedures. As a result, the reported CIs reflect only sampling variability and may not capture the full uncertainty inherent in the original GBD data.

Joinpoint regression

Joinpoint regression analysis was conducted to estimate the average annual percent change (AAPC) and assess long-term trends at both the global and Socio-demographic Index (SDI) levels. The maximum number of joinpoints was set at five (six-line segments) to ensure sufficient model flexibility while preventing overfitting. This upper limit was chosen to balance trend detection sensitivity and statistical robustness, avoiding excessive responsiveness to short-term fluctuations[16].

The Monte Carlo permutation test was applied to determine the actual number of joinpoints, minimizing the sum of squared errors while adjusting for multiple testing. To ensure stable trend estimation, a parametric method was used to compute the annual percent change (APC) and AAPC[17]. The sensitivity analyses and model fit statistics are provided in supplementary Sect. 4.

Cross-country inequalities analysis

SDI is a measure of socio-economic development based on income per capita, average years of schooling for females under 25, and fertility rates. Countries are ranked by SDI from lowest to highest on a scale from 0 to 1. The SDI values are categorized into five levels: low SDI (0–0.455), low-middle SDI (0.455–0.608), middle SDI (0.608–0.690), high-middle SDI (0.690–0.805), and high SDI (0.805–1.0)[12].

To quantify inequalities in the distribution of disability-adjusted life years across countries ranked by their SDI, we employed the Slope Index of Inequality (SII) and the Relative Concentration Index (RCI).

SII measures absolute inequality in disability-adjusted life years by comparing the rates between the most and least advantaged countries along the SDI spectrum. It assumes a linear relationship between disability-adjusted life years and SDI, meaning health burdens increase or decrease in a predictable way as SDI changes. Additionally, SII incorporates population size, ensuring that the results reflect true health disparities across countries of different sizes. RCI focuses on relative inequality, measuring how DALYs are distributed across SDI groups in proportion to their population size. It normalizes the data to show whether DALYs are disproportionately concentrated in either high-SDI or low-SDI countries. RCI assumes that SDI rankings represent socio-economic hierarchies and adjusts for population size to make comparisons more accurate, accounting for the differences in country sizes[18].

The SII was calculated using a repeated iterative weighted least squares model in R. The model was fitted with the rlm function from the MASS package, which accounts for heteroscedasticity in the data. The RCI was calculated using the conindex command in Stata[19, 20]. Detailed explanations of SII, RCI, and SDI ranking can be found in the supplement materials Sect. 5.

Spearman correlation and regression analysis

To examine the relationship between disability-adjusted life years and SDI at the country level, we calculated Spearman correlation coefficients to determine the strength and direction of the non-linear relationship between these variables. Additionally, we applied locally estimated scatterplot smoothing (LOESS) regression to visualize the trend in disability-adjusted life years across the SDI spectrum.

Predictive analysis

To forecast the age-standardized incidence rate from 2022 to 2045, we employed a Bayesian generalized age-period-cohort (BAPC) power model. Model parameters were estimated within a Bayesian inference framework, incorporating the Iterative Leave-out-Node Approach (ILNA) to enhance prediction accuracy[21]. We specified a second-order random walk (RW2) for both period and cohort effects to allow flexible temporal trends, and used Penalized Complexity (PC) priors on the precision parameters to control smoothness. The age effect was modeled as a fixed categorical factor. Sensitivity analyses were conducted to assess the robustness of model results to different prior distributions and smoothness assumptions. The RW2 model with a PC prior (0.5, 0.05) was adopted for final projections.

The estimated parameters were applied to Global Burden of Disease (GBD) Study population projections to predict age-standardized rates through 2045. Credible intervals (CIs) were derived using Integrated Nested Laplace Approximations (INLA), with the 2.5 th and 97.5 th percentiles defining the 95% CI.

Statistical analysis and data visualization

Most statistical analyses and data visualization were conducted using R (version 4.3.3; R Foundation for Statistical Computing, Vienna, Austria). Joinpoint Trend Analysis software (version 5.2.0.0; National Cancer Institute, Rockville, MD, USA) was employed for trend analysis. The epitools (version 0.5–10.1) was used for age-standardized rate calculations, while INLA (version 23.09.09) and BAPC (version 0.0.36) were applied for BAPC projections. MASS package (version 7.3–60.0.1) was used to calculate SII, and Stata Statistical Software: Release 16 (StataCorp, 2019) was used for calculating RCI.A statistical significance threshold of $p < 0.05$ was applied across all analyses.

Results

Global and SDI trends

The total number of pediatric urolithiasis cases increased from 1,355,161 (95% UI: 661,574–2,270,002) in 1990 to 1,562,095 (95% UI: 776,852–2,568,885) in 2021. However, the age-standardized incidence rate decreased slightly from 79 per 100,000 (95% CI: 38–132) in 1990 to 75 per 100,000 (95% CI: 37–124) in 2021. The average annual percent change (AAPC) for age-standardized incidence rate was − 0.138 (95% CI: − 0.183, − 0.093), indicating a slight decline in the global incidence rate over the study period (Table 1, Fig. 1A).Across Socio-Demographic Index (SDI) regions, the sharpest decline in the age-standardized incidence rate was observed in high SDI regions, where it dropped from 60 per 100,000 (95% CI: 28–102) in 1990 to 49 per 100,000 (95% CI: 25–78) in 2021 (AAPC: − 0.690). In contrast, the smallest decrease occurred in low SDI regions, where the age-standardized incidence rate declined from 82 per 100,000 (95% CI: 40–137) to 79 per 100,000 (95% CI: 38–133) (AAPC: − 0.105) (Table 1, Fig. 1A).

Although this long-term downward trend is evident, Fig. 1A reveals that the age-standardized incidence rate exhibited noticeable fluctuations after 2009, particularly at the global level and across multiple SDI regions. The global age-standardized incidence rate initially declined but demonstrated an upward fluctuation after 2009. A similar pattern was observed in the high SDI, high-middle SDI, middle SDI, and low-middle SDI regions, where the age-standardized incidence rate initially followed a downward trajectory but subsequently experienced fluctuations after 2009 (Fig. 1A).

Between 1990 and 2021, the global age-standardized disability-adjusted life years rate showed a consistent decline, decreasing from 1.09 per 100,000 (95% CI: 0.57–2.17) in 1990 to 0.54 per 100,000 (95% CI: 0.29–1.26) in 2021 (AAPC: − 2.244, 95% CI: − 2.351 to − 2.137) (Table 2, Fig. 1B). Unlike the age-standardized incidence rate, which exhibited fluctuations after 2009, the global disability-adjusted life years rate maintained a relatively stable downward trajectory throughout the study period (Fig. 1B) . Across socio-demographic index regions, the largest decline in the disability-adjusted life years rate was observed in middle SDI regions, where it decreased from 1.27 per 100,000 (95% CI: 0.59–1.80) in 1990 to 0.38 per 100,000 (95% CI: 0.24–0.62) in 2021 (AAPC: − 3.843). In contrast, the smallest decrease occurred in high SDI regions, where the disability-adjusted life years rate declined from 0.26 per 100,000 (95% CI: 0.16–0.40) to 0.18 per 100,000 (95% CI: 0.11–0.29) (AAPC: − 1.175).

Region-level differences

In 2021, the age-standardized incidence rate of pediatric urolithiasis varied across regions (Table 1). The highest rate was recorded in Central Asia 178 per 100,000 (95% CI: 95–288), while the lowest rate was observed in East Asia 26 per 100,000 (95% CI: 11–45). Between 1990 and 2021, the age-standardized incidence rate declined in 12 regions, with the steepest decrease in East Asia (AAPC: − 1.78). In contrast, 9 regions exhibited an increasing trend, with Tropical Latin America showing the fastest growth (AAPC: 0.600) (Table 1).

The age-standardized disability-adjusted life years rate also showed substantial regional variation (Table 2). The highest burden was observed in Western Sub-Saharan Africa, reaching 1.58 per 100,000 (95% CI: 0.50–6.19), while the lowest burden was recorded in Australasia, at 0.08 per 100,000 (95% CI: 0.03–0.15). Over the period 1990 to 2021, disability-adjusted life years decreased in 18 regions, with the largest decline in East Asia (AAPC: − 7.130). Conversely, disability-adjusted life years increased in 3 regions, with Tropical Latin America experiencing the most pronounced rise (AAPC: 0.570) (Table 2).

National variations

In 2021, the age-standardized incidence rate of pediatric urolithiasis showed significant variation across countries (Fig. 2 A). The highest age-standardized incidence rate was observed in Armenia, with 250 per 100,000 (95% CI: 140–391), while the lowest age-standardized incidence rate was recorded in Cyprus, at 23 per 100,000 (95% CI:

Table 1 Global and regional incidence of pediatric urolithiasis and average annual percent change from 1990 to 2021

Category	1990 Number	1990 ASIR	2021 Number	2021 ASIR	1990–2021 AAPC
Global	1355161 (661574,2270002)	79 (38,132)	1562095 (776852,2568885)	75 (37,124)	− 0.138 (− 0.183,− 0.093)
Male	772286 (381433,1295780)	87 (43,147)	920741 (464638,1497649)	86 (43,140)	− 0.053 (− 0.090,− 0.016)
Female	582874 (278699,979534)	69 (33,117)	641354 (309106,1070124)	64 (31,107)	− 0.274 (− 0.317,− 0.231)
High SDI	114847 (53872,194155)	60 (28,102)	88404 (44696,141716)	49 (25,78)	− 0.690 (− 0.784,− 0.596)
High-middle SDI	230670 (112665,383824)	83 (40,138)	167914 (85909,274048)	69 (35,113)	− 0.578 (− 0.627,− 0.529)
Middle SDI	414769 (199300,703263)	72 (34,121)	407776 (203882,672071)	69 (34,114)	− 0.125 (− 0.190,− 0.059)
Low-middle SDI	419168 (207524,700220)	92 (45,153)	536926 (263433,883686)	90 (44,148)	− 0.067 (− 0.073,− 0.060)
Low SDI	174123 (84625,292286)	82 (40,137)	359831 (173873,602503)	79 (38,133)	− 0.105 (− 0.113,− 0.096)
Andean Latin America	8436 (3939,14442)	57 (27,98)	11078 (5776,17987)	60 (31,98)	0.179(0.155,0.203)
Australasia	1342 (512,2416)	29 (11,51)	1575 (588,2831)	26 (10,47)	− 0.265(− 0.298,− 0.232)
Caribbean	7667 (3588,13041)	68 (32,115)	8071 (3784,13863)	69 (32,118)	0.046(0.021,0.070)
Central Asia	42291 (22421,68550)	177 (94,286)	48213 (25735,78176)	178 (95,288)	0.023(0.007,0.038)
Central Europe	61206 (32635,98926)	196 (105,317)	32207 (18533,49659)	173 (100,268)	− 0.399(− 0.487,− 0.311)
Central Latin America	57595 (29008,96930)	90 (45,151)	55176 (29188,90036)	84 (45,137)	− 0.237(− 0.358,− 0.117)
Central Sub-Saharan Africa	15211 (7041,26306)	66 (31,113)	38288 (17964,65875)	66 (31,114)	0.042(0.024,0.061)
East Asia	148898 (61860,267116)	45 (19,81)	71267 (31520,123614)	26 (11,45)	− 1.78(− 1.931,− 1.629)
Eastern Europe	95436 (50594,155335)	183 (97,297)	67189 (35231,109642)	176 (93,288)	− 0.113(− 0.137,− 0.088)
Eastern Sub-Saharan Africa	63139 (30067,106611)	75 (36,126)	131558 (62552,221688)	74 (35,125)	− 0.020(− 0.031,− 0.009)
High-income Asia Pacific	28396 (13301,47882)	74 (35,126)	14695 (7052,24544)	61 (29,102)	− 0.644(− 0.749,− 0.540)
High-income Asia Pacific	30,579 (13,200,54,063)	49 (21,87)	32752 (17024,51740)	47 (24,74)	− 0.300(− 0.773,0.176)
North Africa and Middle East	101153 (48509,170518)	74 (35,124)	138042 (65816,231706)	74 (35,124)	− 0.002(− 0.010,0.007)
Oceania	1242 (545,2163)	48 (21,83)	2467 (1095,4303)	50 (22,88)	0.170(0.162,0.178)
South Asia	464223 (232007,771720)	110 (55,183)	592499 (296085,973492)	110 (55,181)	− 0.009(− 0.024,0.006)
Southeast Asia	97829 (44049,169415)	57 (26,98)	90470 (41915,153823)	51 (23,86)	− 0.341(− 0.396,− 0.287)
Southern Latin America	9568 (4446,16397)	63 (29,109)	10836 (5697,17522)	70 (37,113)	0.306(0.271,0.342)
Southern Sub-Saharan Africa	18183 (8853,30436)	89 (43,149)	22185 (10822,36961)	90 (44,150)	0.032(0.014,0.049)
Tropical Latin America	23,172 (10,905,38,445)	42 (20,70)	25521 (12636,42038)	50 (25,82)	0.598(0.437,0.759)
Western Europe	24121 (9895,42309)	32 (13,57)	23088 (10323,38850)	32 (14,54)	− 0.023(− 0.093,0.047)
Western Sub-Saharan Africa	55472 (26060,94525)	69 (32,116)	144919 (68567,245024)	70 (33,118)	0.057(0.034,0.080)

Number is presented with 95% uncertainty intervals (UI), while ASIR (per 100,000) and AAPC are presented with 95% confidence intervals (CI)

Abbreviations: *ASIR* Age-standardized incidence rate, *AAPC* Average annual percent change, *SDI* Socio-demographic index

8–44). From 1990 to 2021, age-standardized incidence rate increased in 147 countries, with the largest increase observed in Spain (AAPC: 1.855). Brunei Darussalam was the only country where age-standardized incidence rate remained unchanged. In contrast, ASIR decreased in 55 countries, with Georgia exhibiting the steepest decline (AAPC: − 2.668) (Fig. 2 B).

The age-standardized disability-adjusted life years rate also demonstrated regional differences (Fig. 2 C). The highest disability-adjusted life years burden was observed in Nigeria, reaching 1.90 per 100,000 (95% CI: 0.55–8.39), while the lowest disability-adjusted life years burden was recorded in New Zealand, at 0.07 per 100,000 (95% CI: 0.03–0.13). Between 1990 and 2021, disability-adjusted life years increased in 46 countries, with Libya showing the largest increase (AAPC: 3.637). Conversely, disability-adjusted life years decreased in 158 countries, with China experiencing the largest decline (AAPC: − 7.235) (Fig. 2 D).

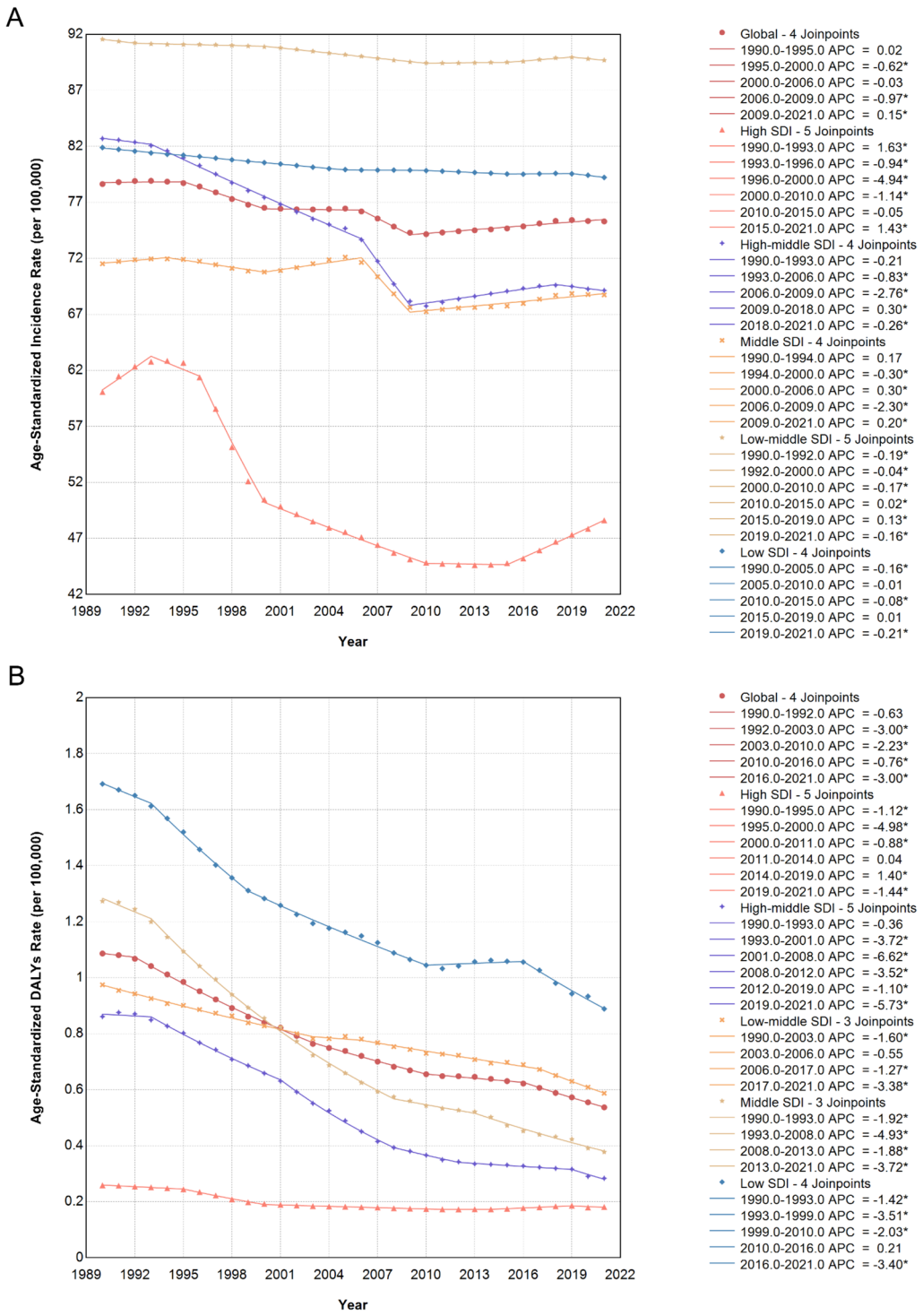

Fig. 1 Trends in age-standardized incidence rates (**A**) and age-standardized disability-adjusted life years rates (**B**) in global and five SDI regions from 1990 to 2021. Abbreviations: DALYs, disability-adjusted life years; SDI, socio-demographic index; APC, annual percent change. *Indicates that the annual percent change is significantly different from zero at the alpha = 0.05 level

Cross-country inequality analysis

Significant cross-country disparities in the burden of pediatric urolithiasis were observed, with higher age-standardized disability-adjusted life years rates concentrated in lower SDI countries (Fig. 3). The Slope Index of Inequality (SII) decreased from 1.44 in 1990 to 0.51 in 2021, while the Concentration Index increased from − 0.15 to − 0.25. SII and

Table 2 Global and regional DALYs of pediatric urolithiasis and average annual percent change from 1990 to 2021

Category	1990 Number	1990 ASR of DALYs	2021 Number	2021 ASR of DALYs	1990–2021 AAPC
Global	18975 (9980,38124)	1.09 (0.57,2.17)	10773 (5944,24663)	0.54 (0.29,1.26)	− 2.244 (− 2.351,− 2.137)
Male	11523 (4254,28318)	1.28 (0.48,3.13)	7421 (3453,19484)	0.72 (0.33,1.94)	− 1.829 (− 1.999,− 1.658)
Female	7453 (2894,12506)	0.88 (0.33,1.47)	3351 (1915,5679)	0.34 (0.19,0.58)	− 3.024 (− 3.201,− 2.846)
High SDI	491 (305,758)	0.26 (0.16,0.40)	329 (194,530)	0.18 (0.11,0.29)	− 1.175(− 1.291,− 1.059)
High-middle SDI	2349 (1462,3263)	0.86 (0.54,1.19)	680 (414,1069)	0.28 (0.17,0.44)	− 3.588(− 3.844,− 3.332)
Middle SDI	7336 (3388,10371)	1.27 (0.,1.80)	2202 (1378,3563)	0.38 (0.24,0.62)	− 3.843(− 4.082,− 3.603)
Low-middle SDI	4633 (1708,9637)	0.97 (0.37,2.01)	3425 (1950,6767)	0.59 (0.33,1.18)	− 1.615(− 1.773,− 1.457)
Low SDI	4157 (744,14582)	1.69 (0.33,5.76)	4131 (1555,12822)	0.89 (0.34,2.73)	− 2.055(− 2.243,− 1.867)
Andean Latin America	42 (20,74)	0.29 (0.13,0.49)	41 (22,69)	0.22 (0.12,0.38)	− 0.786(− 1.078,− 0.493)
Australasia	4 (2,8)	0.10 (0.04,0.18)	5 (2,9)	0.08 (0.03,0.15)	− 0.699(− 0.849,− 0.549)
Caribbean	48 (18,121)	0.42 (0.15,1.04)	41 (16,95)	0.35 (0.14,0.83)	− 0.489(− 0.678,− 0.299)
Central Asia	330 (188,501)	1.32 (0.75,1.99)	241 (154,368)	0.88 (0.56,1.34)	− 1.266(− 1.741,− 0.787)
Central Europe	270 (180,405)	0.87 (0.58,1.30)	96 (52,163)	0.52 (0.28,0.87)	− 1.653(− 1.823,− 1.483)
Central Latin America	478 (367,635)	0.74 (0.57,0.99)	245 (158,381)	0.37 (0.24,0.58)	− 2.233(− 2.627,− 1.837)
Central Sub-Saharan Africa	127 (35,385)	0.49 (0.15,1.40)	165 (82,309)	0.28 (0.14,0.53)	− 1.722(− 1.766,− 1.678)
East Asia	5564 (2132,8120)	1.69 (0.65,2.46)	480 (290,751)	0.18 (0.11,0.28)	− 7.131(− 7.586,− 6.674)
Eastern Europe	415 (276,624)	0.80 (0.53,1.20)	225 (127,371)	0.59 (0.33,0.98)	− 0.962(− 1.172,− 0.751)
Eastern Sub-Saharan Africa	871 (210,2115)	0.93 (0.24,2.21)	765 (436,1390)	0.43 (0.25,0.78)	− 2.456(− 2.582,− 2.330)
High-income Asia Pacific	92 (46,158)	0.24 (0.12,0.42)	47 (24,81)	0.20 (0.10,0.34)	− 0.673(− 0.901,− 0.445)
High-income Asia Pacific	119 (68,196)	0.19 (0.11,0.32)	134 (87,208)	0.19 (0.12,0.30)	− 0.014(− 0.361,0.335)
North Africa and Middle East	1922 (794,2961)	1.36 (0.57,2.09)	1112 (530,1681)	0.60 (0.29,0.91)	− 2.591(− 2.704,− 2.479)
Oceania	4 (2,7)	0.15 (0.06,0.28)	7 (3,14)	0.15 (0.07,0.28)	0.037(− 0.008,0.082)
South Asia	4065 (1389,6936)	0.94 (0.33,1.60)	2702 (1550,4267)	0.51 (0.29,0.81)	− 1.902(− 2.086,− 1.719)
Southeast Asia	903 (432,1480)	0.53 (0.25,0.87)	549 (319,829)	0.31 (0.18,0.47)	− 1.709(− 1.941,− 1.477)
Southern Latin America	29 (14,52)	0.19 (0.09,0.34)	33 (17,58)	0.21 (0.11,0.37)	0.309(0.107,0.510)
Southern Sub-Saharan Africa	107 (45,204)	0.52 (0.22,0.98)	96 (54,156)	0.39 (0.22,0.64)	− 0.868(− 1.276,− 0.458)
Tropical Latin America	139 (95,207)	0.26 (0.17,0.38)	156 (113,221)	0.31 (0.22,0.43)	0.569(0.319,0.820)
Western Europe	120 (77,181)	0.16 (0.11,0.25)	91 (53,149)	0.13 (0.07,0.21)	− 0.853(− 1.043,− 0.663)
Western Sub-Saharan Africa	3327 (501,16045)	3.35 (0.55,15.85)	3540 (1093,14031)	1.58 (0.50,6.19)	− 2.407(− 2.648,− 2.166)

Number is presented with 95% uncertainty intervals (UI), while age-standardized DALYs (per 100,000) and AAPC are presented with 95% confidence intervals (CI)

Abbreviations: *ASR* Age-standardized rate, *DALYs* Disability-adjusted life years, *AAPC* Average annual percent change, *SDI* Socio-demographic index

RCI values can be found in the supplementary materials Sect. 5.

Spearman correlation and regression analysis

Spearman correlation analysis and LOESS regression indicated a negative association between SDI and age-standardized disability-adjusted life years rates ($\rho = -0.53$, $p <$ 0.001) (Supplementary Materials S1 - 2). Countries with the highest age-standardized disability-adjusted life years rates in 2021 included Nigeria (1.90, 95% CI: 0.55–8.39), Chad (1.74, 95% CI: 0.30–7.01), and Tajikistan (1.70, 95% CI: 0.78–3.17). The lowest disability-adjusted life years rates were observed in New Zealand (0.07, 95% CI: 0.03–0.13), Australasia (0.08, 95% CI: 0.03–0.15), and Monaco (0.08, 95% CI: 0.03–0.16).

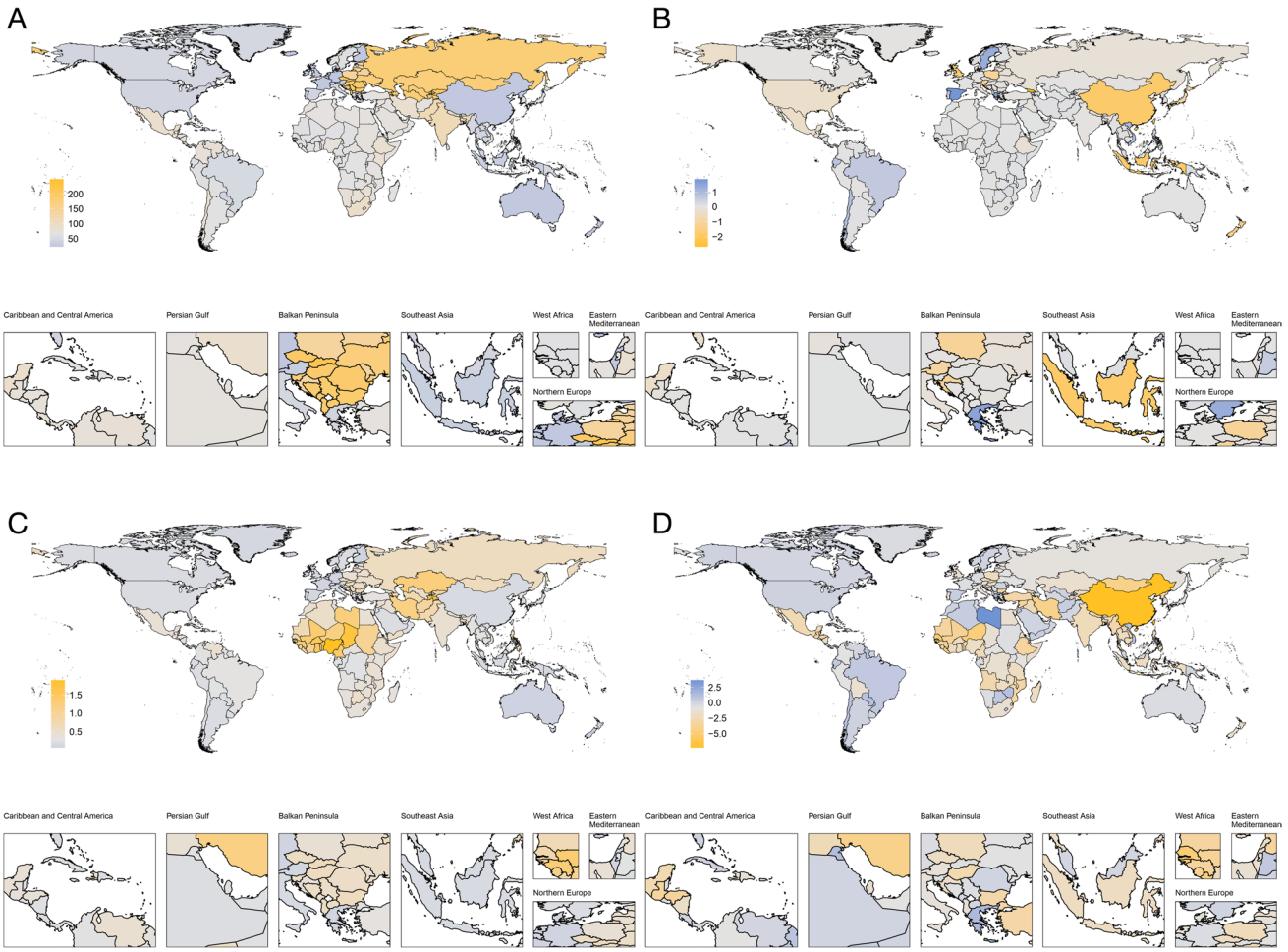

Fig. 2 The age-standardized incidence rates (**A**) and disability-adjusted life years rates (**C**) of pediatric urolithiasis in 2021. The average annual percent change of age-standardized incidence rates (**B**) and disability-adjusted life years rates (**D**) from 1990 to 2021. Enlarged versions of Panels A–D are provided in supplementary Sect. 7 for improved clarity

Predicted trends

Using Bayesian Age-Period-Cohort (BAPC) models, the projected global age-standardized incidence rate for 2022–2045 is shown in Fig. 4. The model predicts a slight increase in age-standardized incidence rate after 2021, with a widening confidence interval beyond 2021. The results of posterior predictive checks and sensitivity analysis can be found in the supplementary Sect. 6.

Discussion

Consistent with previous studies, our findings reveal a declining trend in the global and regional age-standardized incidence rate (ASIR) and disability-adjusted life years (DALYs) for pediatric urolithiasis between 1990 and 2021[10]. However, the total number of cases has risen, especially in low and low-middle Socio-Demographic Index (SDI) regions, likely due to population growth and changing epidemiology.

We also observed fluctuating increases in the age-standardized incidence rate after 2009 in high, high-middle, and middle SDI regions. Initially, we thought this trend might be linked to guidelines recommending ultrasound as the first-line imaging method for pediatric urolithiasis and more frequent use of CT scans[3, 22]. However, previous studies indicate that in the United States, CT utilization rates increased before 2009 and peaked in 2007[23, 24], while ultrasound usage increased after 2009, but no study has definitively demonstrated that this increase contributed to a rise in symptomatic incidence of pediatric urolithiasis[25]. Therefore, this hypothesis may not be entirely reliable, and the underlying causes warrant further investigation.

Our Bayesian Age-Period-Cohort (BAPC) model projects a gradual increase in the age-standardized incidence rate (ASIR) from 2022 to 2045. This trend is most evident

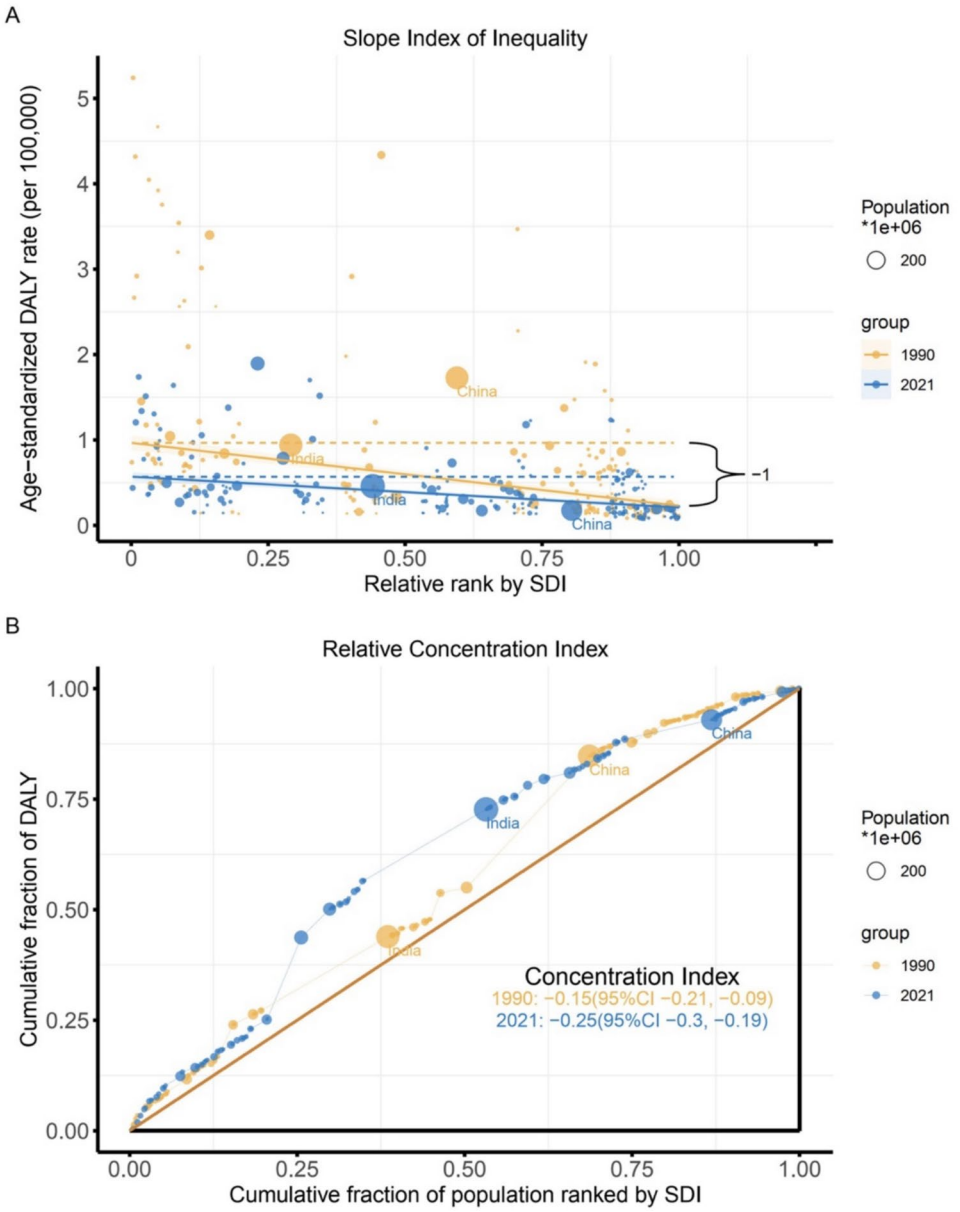

Fig. 3 (**A**) Slope index of inequality (SII) for disability-adjusted life years by SDI Rank in 1990 and 2021. (**B**) Relative concentration index (RCI) of disability-adjusted life years by cumulative population rank in 1990 and 2021

under models with second-order random walks (RW2), which allow for smoother acceleration over time, and may reflect the cumulative effects of population aging, evolving risk exposures, and improved diagnostic sensitivity. In contrast, models with first-order random walks (RW1) tended to produce flatter projections, suggesting greater prior-driven constraint on long-term trend dynamics. Given the inherent uncertainty in long-term forecasting, we performed sensitivity analyses using different prior distributions and smoothness assumptions. Despite some variation in uncertainty bounds, the RW2 models, particularly those with a penalized complexity (PC) prior of (0.5, 0.05), demonstrated relatively better model fit.

Significant regional differences in age-standardized incidence rate exist, likely due to environmental and socioeconomic factors like temperature, diet, and water quality [26–30]. Interestingly, our analysis showed a negative correlation between age-standardized incidence rate and SDI, contrary to the slight positive correlation typically found in all age groups[31–33]. This indicates that the causes of pediatric urolithiasis may differ from those in adults, highlighting the need for age-specific prevention and management.

The disability-adjusted life years burden is heavily concentrated in low and low-middle SDI regions, pointing to significant health disparities. While absolute health inequality has decreased, relative inequality has grown, meaning

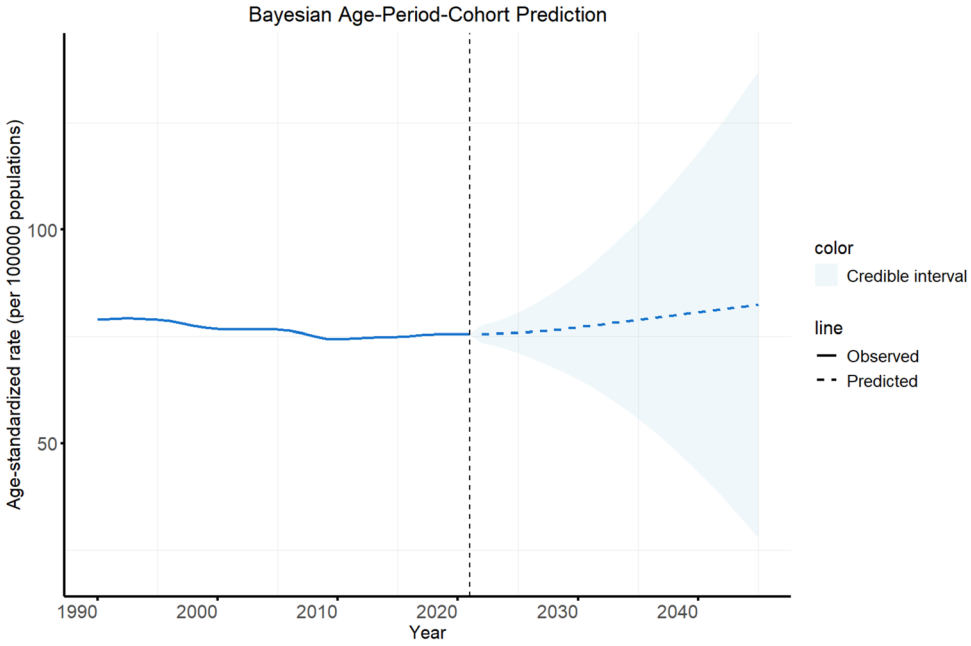

Fig. 4 The global trends in the age-standardized incidence rate of pediatric urolithiasis from 1990 to 2021, with projected trends from 2022 to 2045

that although global health has improved, the gap between high- and low-SDI regions has widened. One possible reason for this disparity is the high recurrence rate and long-term renal complications in children[34]. These factors emphasize that managing pediatric urolithiasis remains a global challenge, particularly in low-SDI countries with limited healthcare infrastructure.

Given these challenges, expanding access to effective treatments is essential to improving outcomes for pediatric urolithiasis patients, especially in resource-limited regions. Among available treatment options, retrograde intrarenal surgery (RIRS) is considered one of the most effective and minimally invasive approaches. Compared to percutaneous nephrolithotomy (PCNL) and extracorporeal shock wave lithotripsy (ESWL), RIRS offers higher stone-free rates, fewer complications, and shorter recovery times, making it especially suitable for pediatric patients[35, 36]. But currently, its use remains limited in low-income countries[37].

To reduce health inequities, future efforts should focus on improving access to minimally invasive techniques, enhancing surgeon training, upgrading healthcare infrastructure, and addressing environmental factors like water supply and nutrition[38]. These strategies will help alleviate the burden of pediatric urolithiasis globally.

This study uses data from the Global Burden of Disease (GBD) database, which, while comprehensive, faces challenges with data accuracy, especially in low-SDI regions, potentially leading to misestimations of the disease burden[39, 40]. Additionally, we could only analyze data from children aged 0–14 years due to GBD limitations, limiting a full understanding of pediatric urolithiasis trends. Future research should include more data from low-SDI regions and consider additional risk factors to enable better-targeted interventions.

In conclusion, this study highlights ongoing disparities in pediatric urolithiasis burden and stresses the importance of focused public health interventions, particularly in low-SDI regions, to improve child health outcomes globally.

Supplementary Information The online version contains supplementary material available at https://doi.org/10.1007/s00431-025-06134-4.

Acknowledgements We would like to express our sincere gratitude to the Global Burden of Disease (GBD) research team for providing access to comprehensive datasets used in this study.

Author contributions Zheng Xu conceptualized the study, provided data visualization, and drafted the manuscript. Tianfu Ding, Daxun Luo and Yang Chen were responsible for data collection and validation. Haifeng Song, Boxing Su and Yubao Liu contributed to the interpretation of results. Bo Xiao and Jianxing Li supervised the project.

Funding This research was conducted without specific funding from any agency in the public, commercial, or not-for-profit sectors. The authors received no financial support for the study design, data collection, analysis, or publication of this work.

Data availability This study relied on publicly available data from the Global Burden of Disease (GBD) 2021 database, accessed through the Global Health Data Exchange (GHDx) query tool (https://ghdx.healthdata.org/). The dataset provides comprehensive estimates of incidence, prevalence, and disability-adjusted life years (DALYs) for pediatric urolithiasis across 204 countries and territories. Detailed descriptions of data collection, processing, and estimation methodologies are available in the GBD study publications cited in the manuscript.

Declarations

Ethics approval This study did not involve patient personal information. The data usage complies with the Institute for Health Metrics and Evaluation ("IHME") Free-of-Charge Non-commercial User Agreement, and no additional ethical approval was required.

Consent to participate Not applicable.

Consent for publication Not applicable.

Competing interests The authors declare no competing interests.

References

1. Tasian GE, Ross ME, Song L, Sas DJ, Keren R, Denburg MR et al (2016) Annual Incidence of Nephrolithiasis among Children and Adults in South Carolina from 1997 to 2012. Clin J Am Soc Nephrol 11(3):488–496. https://doi.org/10.2215/CJN.07610715
2. Van Batavia JP, Tasian GE (2016) Clinical effectiveness in the diagnosis and acute management of pediatric nephrolithiasis. Int J Surg 36(Pt D):698–704. https://doi.org/10.1016/j.ijsu.2016.11.030
3. Dwyer ME, Krambeck AE, Bergstralh EJ, Milliner DS, Lieske JC, Rule AD (2012) Temporal trends in incidence of kidney stones among children: a 25-year population based study. J Urol 188(1):247–252. https://doi.org/10.1016/j.juro.2012.03.021
4. Cao B, Daniel R, McGregor R, Tasian GE (2023) Pediatric Nephrolithiasis. Healthcare (Basel). 11(4):552. https://doi.org/10.3390/healthcare11040552
5. Sorokin I, Mamoulakis C, Miyazawa K, Rodgers A, Talati J, Lotan Y (2017) Epidemiology of stone disease across the world. World J Urol 35(9):1301–1320. https://doi.org/10.1007/s00345-017-2008-6
6. Ciongradi CI, Filip F, Sârbu I, Iliescu Halițchi CO, Munteanu V, Candussi I-L (2022) The Impact of Water and Other Fluids on Pediatric Nephrolithiasis. Nutrients 14(19). https://doi.org/10.3390/nu14194161
7. Routh JC, Graham DA, Nelson CP (2010) Epidemiological trends in pediatric urolithiasis at United States freestanding pediatric hospitals. J Urol 184(3):1100–1104
8. Orta-Sibu N, Lopez M, Moriyon JC, Chavez JB (2002) Renal diseases in children in Venezuela. South America Pediatr Nephrol 17(7):566–569
9. Lagomarsino E, Avila D, Baquedano P, Cavagnaro SMF, Céspedes P (2003) Litiasis urinaria en pediatría. Rev Chil Pediatr 74(4):381–388
10. Awedew AF et al (2024) The global, regional, and national burden of urolithiasis in 204 countries and territories, 2000–2021: a systematic analysis for the Global Burden of Disease Study 2021. EClinicalMedicine 78:102924. https://doi.org/10.1016/j.eclinm.2024.102924
11. Naghavi M et al (2024) Global burden of 288 causes of death and life expectancy decomposition in 204 countries and territories and 811 subnational locations, 1990–2021: a systematic analysis for the Global Burden of Disease Study 2021. Lancet (London, England) 403(10440):2100–32. https://doi.org/10.1016/S0140-6736(24)00367-2
12. Ferrari AJ et al (2024) Global incidence, prevalence, years lived with disability (YLDs), disability-adjusted life-years (DALYs), and healthy life expectancy (HALE) for 371 diseases and injuries in 204 countries and territories and 811 subnational locations, 1990-2021: a systematic analysis for the Global Burden of Disease Study 2021. Lancet (London, England) 403(10440):2133–61. https://doi.org/10.1016/S0140-6736(24)00757-8
13. Selvin S (2004) Statistical Analysis of Epidemiologic Data. Oxford University Press
14. Anderson RN, Rosenberg HM (1998) Age standardization of death rates: implementation of the year 2000 standard. Natl Vital Stat Rep 47(3)
15. Fay MP, Feuer EJ (1997) Confidence intervals for directly standardized rates: a method based on the gamma distribution. Stat Med 16(7):791–801
16. Zhai Z, Zheng Y, Li N, Deng Y, Zhou L, Tian T et al (2020) Incidence and disease burden of prostate cancer from 1990 to 2017: Results from the Global Burden of Disease Study 2017. Cancer 126(9):1969–1978. https://doi.org/10.1002/cncr.32733
17. Institute NC: Joinpoint Trend Analysis Software. https://surveillance.cancer.gov/joinpoint/ Accessed 2024/09/03.
18. Organization WH (2013) Handbook on health inequality monitoring: with a special focus on low-and middle-income countries. World Health Organization
19. Erreygers G, Clarke P, Van Ourti T (2012) "Mirror, mirror, on the wall, who in this land is fairest of all?" Distributional sensitivity in the measurement of socioeconomic inequality of health. J Health Econ 31(1):257–270. https://doi.org/10.1016/j.jhealeco.2011.10.009
20. O'Donnell O, O'Neill S, Van Ourti T, Walsh B (2016) conindex: Estimation of concentration indices. Stata Journal 16(1):112–138. https://doi.org/10.1177/1536867x1601600112
21. Jürgens V, Ess S, Cerny T, Vounatsou P (2014) A Bayesian generalized age-period-cohort power model for cancer projections. Stat Med 33(26):4627–4636. https://doi.org/10.1002/sim.6248
22 Riccabona M, Avni FE, Blickman JG, Dacher J-N, Darge K, Lobo ML et al (2009) Imaging recommendations in paediatric uroradiology. Minutes of the ESPR uroradiology task force session on childhood obstructive uropathy, high-grade fetal hydronephrosis, childhood haematuria, and urolithiasis in childhood. ESPR Annual Congress, Edinburgh, UK, June 2008. Pediatr Radiol. 39(8):891–8. https://doi.org/10.1007/s00247-009-1233-6
23. Niles LM, Goyal MK, Badolato GM, Chamberlain JM, Cohen JS (2017) US Emergency Department Trends in Imaging for Pediatric Nontraumatic Abdominal Pain. Pediatrics 140(4). https://doi.org/10.1542/peds.2017-0615.
24. Tasian GE, Pulido JE, Keren R, Dick AW, Setodji CM, Hanley JM et al (2014) Use of and regional variation in initial CT imaging for kidney stones. Pediatrics 134(5):909–915. https://doi.org/10.1542/peds.2014-1694
25. Ziemba JB, Canning DA, Lavelle J, Kalmus A, Tasian GE (2015) Patient and institutional characteristics associated with initial computerized tomography in children presenting to the emergency department with kidney stones. J Urol 193(5 Suppl):1848–1853. https://doi.org/10.1016/j.juro.2014.09.115

26. Ong KL, Stafford LK, McLaughlin SA, Boyko EJ, Vollset SE, Smith AE et al (2023) Global, regional, and national burden of diabetes from 1990 to 2021, with projections of prevalence to 2050: a systematic analysis for the Global Burden of Disease Study 2021. The Lancet 402(10397):203–234
27. Dai X, Gakidou E, Lopez AD (2022) Evolution of the global smoking epidemic over the past half century: strengthening the evidence base for policy action. Tob Control 31(2):129–137. https://doi.org/10.1136/tobaccocontrol-2021-056535
28. Afshin A, Forouzanfar M, Reitsma M, Sur P, Estep K, Lee A, et al (2017) Health effects of overweight and obesity in 195 countries over 25 years 377. https://org/101056/NEJMoa1614362, https://wwwncbinlmnihgov/pubmed/28604169.13-27
29. Sas DJ (2011) An update on the changing epidemiology and metabolic risk factors in pediatric kidney stone disease. Clin J Am Soc Nephrol 6(8):2062–2068. https://doi.org/10.2215/CJN.11191210
30. Pettifor JM (2014) Calcium and Vitamin D Metabolism in Children in Developing Countries. Ann Nutr Metab 64:15–22
31. Li S, Huang X, Liu J, Yue S, Hou X, Hu L et al (2022) Trends in the Incidence and DALYs of Urolithiasis From 1990 to 2019: Results From the Global Burden of Disease Study 2019. Front Public Health 10:825541. https://doi.org/10.3389/fpubh.2022.825541
32. Zhang L, Zhang X, Pu Y, Zhang Y, Fan J (2022) Global, Regional, and National Burden of Urolithiasis from 1990 to 2019: A Systematic Analysis for the Global Burden of Disease Study 2019. Clin Epidemiol 14:971–983. https://doi.org/10.2147/CLEP.S370591
33. Zi H, Liu M-Y, Luo L-S, Huang Q, Luo P-C, Luan H-H et al (2024) Global burden of benign prostatic hyperplasia, urinary tract infections, urolithiasis, bladder cancer, kidney cancer, and prostate cancer from 1990 to 2021. Mil Med Res 11(1):64. https://doi.org/10.1186/s40779-024-00569-w
34. Baştuğ F, Düşünsel R (2012) Pediatric urolithiasis: causative factors, diagnosis and medical management. Nat Rev Urol 9:138–146
35 Saad KSM, Youssif ME, Al Islam Nafis Hamdy S, Fahmy A, El Din Hanno AG, El-Nahas AR (2015) Percutaneous Nephrolithotomy vs Retrograde Intrarenal Surgery for Large Renal Stones in Pediatric Patients: A Randomized Controlled Trial. J Urol 194(6):1716–20. https://doi.org/10.1016/j.juro.2015.06.101
36. Baş O, Dede O, Aydogmus Y, Utangaç M, Yikilmaz TN, Damar E et al (2016) Comparison of Retrograde Intrarenal Surgery and Micro-Percutaneous Nephrolithotomy in Moderately Sized Pediatric Kidney Stones. J Endourol 30(7):765–770. https://doi.org/10.1089/end.2016.0043
37. Raheem OA, Khandwala YS, Sur RL, Ghani KR, Denstedt JD (2017) Burden of Urolithiasis: Trends in Prevalence, Treatments, and Costs. Eur Urol Focus 3(1):18–26. https://doi.org/10.1016/j.euf.2017.04.001
38. Injeyan M, Bidault V, Bacchetta J, Bertholet-Thomas A (2023) Hydration and Nephrolithiasis in Pediatric Populations: Specificities and Current Recommendations. Nutrients 15(3). https://doi.org/10.3390/nu15030728
39. Murray CJL et al (2020) Global burden of 87 risk factors in 204 countries and territories, 1990–2019: a systematic analysis for the Global Burden of Disease Study 2019. Lancet (London, England) 396(10258):1223–49. https://doi.org/10.1016/S0140-6736(20)30752-2
40. Vos T et al (2020) Global burden of 369 diseases and injuries in 204 countries and territories, 1990–2019: a systematic analysis for the Global Burden of Disease Study 2019. Lancet (London, England). 396(10258):1204–22. https://doi.org/10.1016/S0140-6736(20)30925-9